Supporting Information for "Evidence of an aseismic slip continuously driving the 2017 Valparaiso earthquake sequence"

L. Moutote[1], Y. Itoh[2], O. Lengliné[1], Z. Duputel[3]and A. Socquet[2]

[1]Institut Terre et Environnement de Strasbourg, UMR7063, Université de Strasbourg/EOST, CNRS, Strasbourg, France.

[2]Université Grenoble Alpes, Université Savoie Mont Blanc, CNRS, IRD, ISTerre, Grenoble, France.

[3]Observatoire Volcanologique du Piton de la Fournaise, Université Paris Cité, Institut de Physique du Globe de Paris, CNRS, F-75005, Paris France.

Contents of this file

Text S1: ETAS-I Synthetic tests To support the significance of the transient seismicity observed in the vicinity of the mainshock in section 3, we perform the same analysis over synthetic catalogs. Synthetic catalogs follow the ETASI model (as defined in the main text), but contains a transient background seismicity somewhere in time in addition to the stationary background rate μ. We generate a synthetic catalogs as follow:

1. We first draw true background events over 5-years from a stationary Poisson process of rate μ.

2. In addition to this stationary background seismicity, we add a transient background seismicity comprising 300 events after a start time T_0. The 300 waiting times after T_0 are drawn from an exponential distribution with an expected value $\lambda = 5$ days.

3. We draw all magnitudes independently from the G-R law.

4. We generate cascade of aftershock sequences for all background events following the ETAS model (Zhuang & Touati, 2015).

5. We build the short-term incompleteness by removing events hidden by T_b (Hainzl, 2021).

The resulting catalog contains magnitude-dependent aftershocks and stationary background events consistent with our ETASI model but also 300 transient background events after T_0. The ETASI parameters $(A, c, p, \alpha, \mu, b, T_b)$ used for the simulations of the stationary background rate and aftershock sequences are the one extracted from ValEqt catalog. We present an example of a synthetic catalog on figure S2.

We perform the same seismicity analysis described in section 3 but with the synthetic catalogs previously generated and try to recover the transient background signal we added. As for ValEqt, we first extract from the synthetic catalogs, the best-fitting parameters

of the ETASI model fixing $\alpha = \beta$. Then, thanks to the transformed time analysis, the synthetic seismicity is tested with respect to predictions. Figure S2.c-d shows that we recover a significant difference between the synthetic seismicity and the best-fitting ETASI prediction, exactly at the time of the transient background rate. We observe the same three regimes of seismicity as observed in the ValEqt analysis: A slight deficit of seismicity for the two time-periods outside of the transient and a significant excess of seismicity within the transient. Note that the number of earthquake in excess is consistent with the 300 transient events added during the simulation. This support the hypothesis that a non-stationary transient background rate can be detected by identifying breaking point in the transformed time analysis. It also shows that a transient background seismicity bias the parameter estimation of the ETASI model. The seismicity outside the transient is in deficit compared to the best-fitting ETASI parameters, even if during these range earthquakes can be fully explain the ETASI parameters extracted from ValEqt. We find that the parameter estimation of A is biased toward a higher value than the one used for the simulation. This is because the model is trying to include a maximum of the non-stationary transient events in the aftershock triggering scheme to reduce at best the seismicity excess. It increases the aftershock productivity of the best-fitting ETASI parameters at the cost of stationary times.

Text S2: MISD synthetic tests Our modified MISD model contain an additional triggering kernel expected to capture earthquakes not explained by a magnitude-dependent triggering scheme. To support our modified MISD model and test its ability to capture the a transient non-stationary seismicity at proximity to the mainshock, we perform the same analysis over synthetic catalogs. We use two sets of synthetic catalogs generated according to the ETAS model:

1. 100 synthetic catalogs containing a transient background seismicity in addition to the stationary background rate.

2. 100 synthetic catalogs with no transient seismicity.

The synthetic catalogs are generated following the method described in ETASI synthetic test section, with or without the transient after T_0. Here, (1) tests the ability of the external triggering kernel to recover a non-stationary transient. (2) ensure that the external kernel don't capture any seismicity when there is no anomaly. For the ValEqt catalog, the start point of the external triggering kernel of the MISD model was a-priory pinned with the start of foreshock sequence to further study the transient seismicity previously highlighted the ETASI analysis. For synthetic catalogs we a-priory pin the transient start point as follow: For (1), the start point of the MISD external triggering kernel is set at the beginning of the transient, as if it was previously detected by an ETASI analysis (see ETASI synthetics test). For (2), as their is no transient, we pin the kernel start 2 days before the largest magnitude of the catalog, to mimic the settings of the Valparaiso foreshock sequence.

We present in Figure S3 the cumulative count of earthquake declustered by the MISD analysis for the 2 test sets . Declustered events include background events and those as-

sociated with the external triggering process. MISD results of the two synthetic case (1) and (2) are present in Figure S3.a and b, respectively. For (1), we shows that the declustering is recovering both stationary background events and the 300 transient background events. For (2), the external kernel do not gather any earthquakes and we only recover the stationary background rate. It shows that the external triggering kernel is only able to extract a seismicity that is not explained by a magnitude-dependent triggering process or a stationary background rate. If the catalog is fully explained by a magnitude-dependent triggering process, the external kernel rate and length reduce to zero.

References

Hainzl, S. (2021). ETAS-Approach Accounting for Short-Term Incompleteness of Earthquake Catalogs. *Bulletin of the Seismological Society of America*. doi: 10.1785/0120210146

Ogata, Y. (1988). Statistical Models for Earthquake Occurrences and Residual Analysis for Point Processes. *Journal of the American Statistical Association*, *83*(401), 9–27. doi: 10.1080/01621459.1988.10478560

Zhuang, J., & Touati, S. (2015). Stochastic simulation of earthquake catalogs. *Community Online Resource for Statistical Seismicity Analysis*, *Theme V*(1), 34.

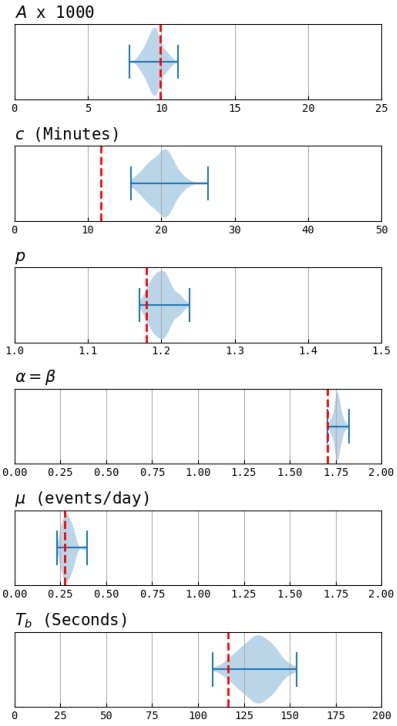

Figure S1. Maximum likelihood estimation of the parameters of 100 synthetic catalogs following the ETASI model. Red vertical dotted lines are the true ETASI parameters used for the generation of the synthetics catalogs.

Table S1. Repeater detection as function of the stress drop used in the circular crack model

Stress Drop $\Delta\sigma$	Number of repeater families	Total number of repeaters
1 MPa	353	1218
3 MPa	352	1211
10 MPa	351	1201

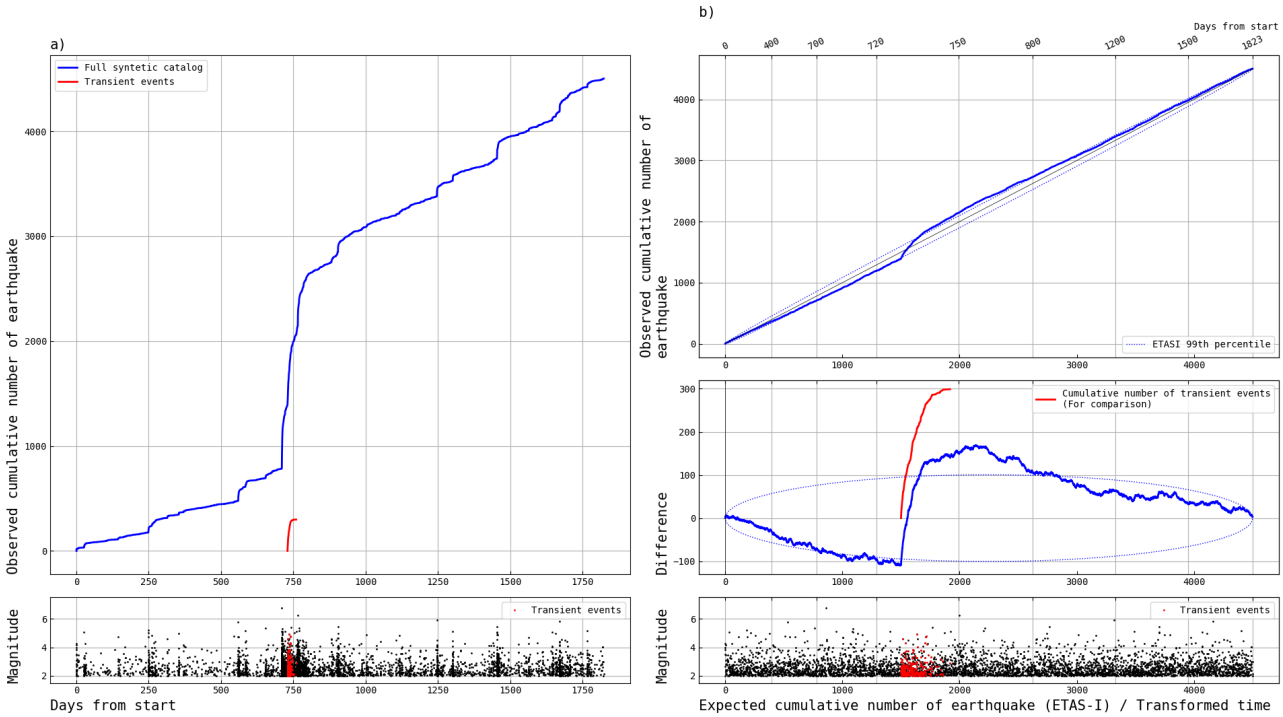

Figure S2. ETASI seismicity analysis over a synthetics catalog following the ETASI model but including a transient non-stationary background rate. (a) (Blue) Time-evolution of the cumulative number of earthquakes in the synthetic catalog. (Red) Cumulative number of the non-stationary background event in the synthetic catalog. Bottom subplot is the time and magnitude of the synthetic catalog. The bottom subplot (black dots) is the time-magnitude evolution of the ValEqt catalog. (b) Cumulative number of earthquakes observed in the synthetic catalog against the cumulative number of earthquakes predicted by the best fitting ETASI model. Blue dotted lines shows the ETASI 99^{th} percentile confidence interval. This x-axis representation of time is knows as the transformed time analysis (Ogata, 1988). The middle subplot is the difference between the observed and expected cumulative number of earthquake in the transformed time domain. (Red) Cumulative number of the non-stationary background event in the transformed time domain. We observe a significant seismicity excess compared to the best fitting ETASI model exactly where we added the transient non-stationary background event. Bottom subplot show the magnitudes of the synthetic catalog in the transformed time domain.

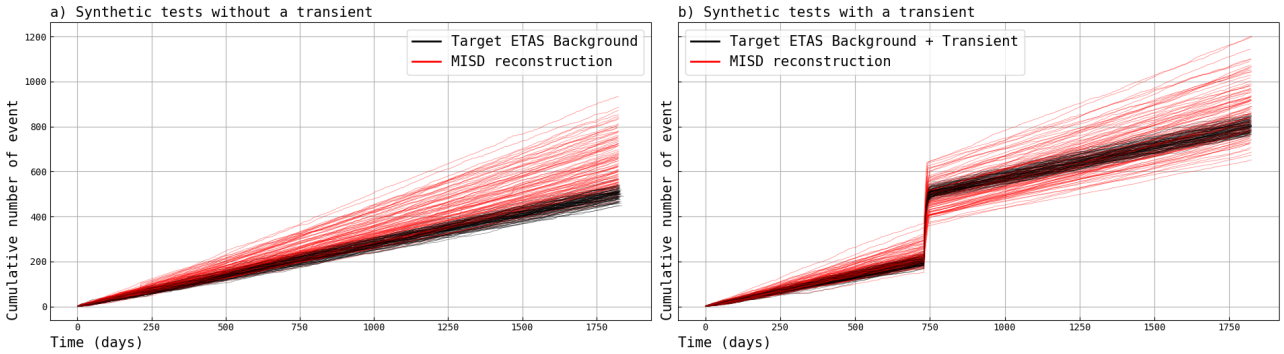

Figure S3. MISD seismicity analysis over 100 synthetics catalog following the ETASI model but including a transient non-stationary background rate. (a) Cumulative number of background earthquake declustered by the MISD procedure over 100 synthetic catalog with no transient. (b) Cumulative number of background earthquake declustered by the MISD procedure over 100 synthetic catalog containing a transient background seismicity. When there is a transient, our MISD model is able to recover both stationary background events and the transient background events. When there is no transient, MISD model is only recover the stationary background events.

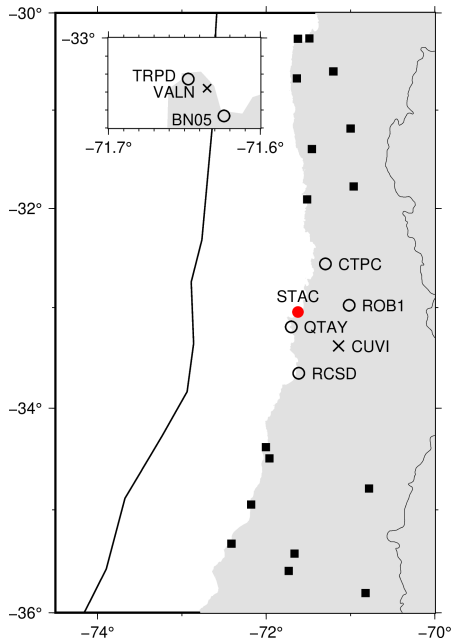

Figure S4. GPS site location (site names labeled). Open circles and crosses indicate sites used and not used for this study, respectively. A red dot indicates a site STAC which is a pseudo-site to represent stacked time series of TRPD and BN05 shown in the inset (See main text and Figures 7, S6, and S7 for details). Solid squares indicate sites used for common mode filter construction.

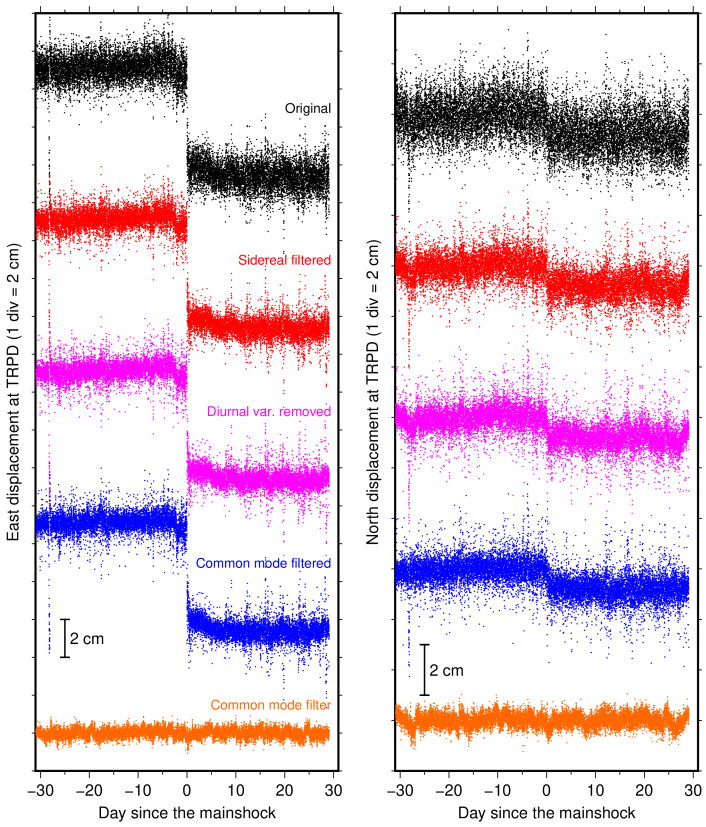

Figure S5. Example of high-rate GPS post-processing at site TRPD (Figure S4) for east (left) and north (right) components. Black dots indicate high-rate GPS coordinates fixed to South American plate reference system. Red, purple, and blue dots indicate those after multipath effects, diurnal variation, and common mode fluctuation removals, respectively (See main text for details). Orange dots indicate a common mode filter.

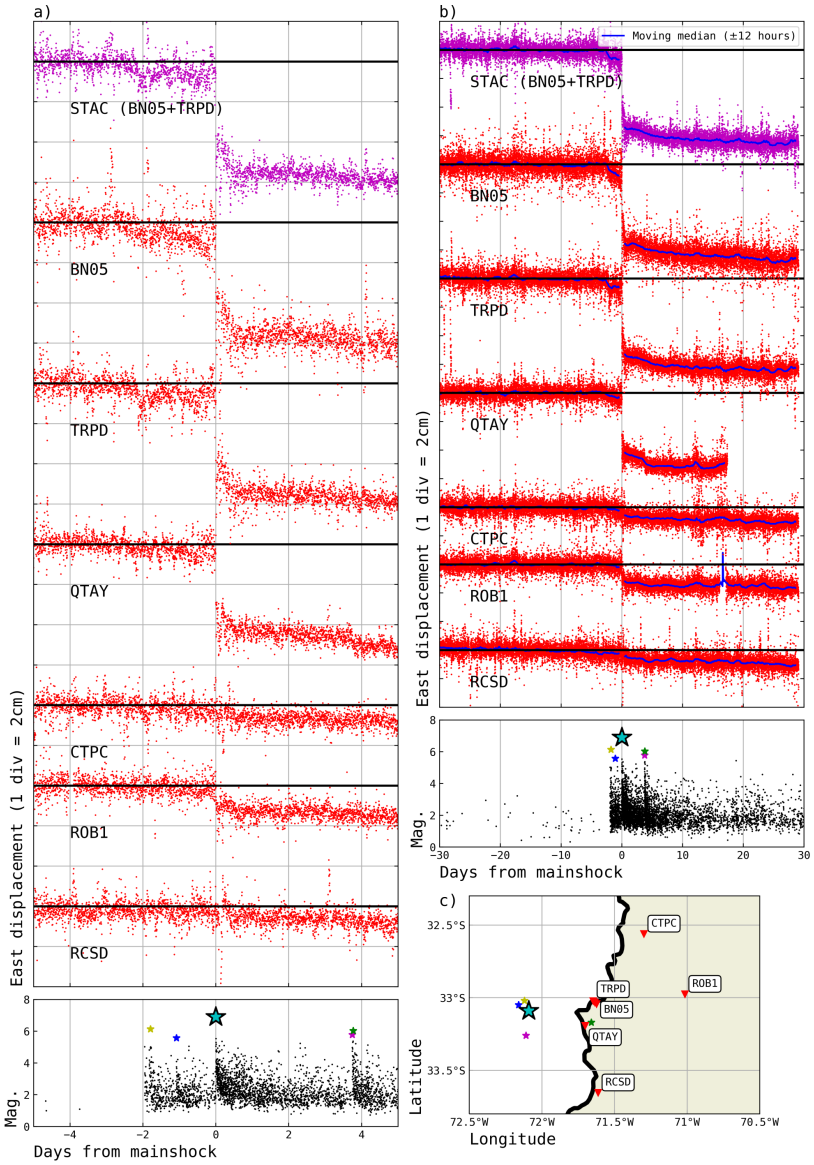

Figure S6. Comparison of high-rate GPS displacements and seismicity evolution before and after the 2017 Valparaiso mainshock. a) Red dots show cleaned east positions between 5 days before and after the mainshock at the two closest sites QTAY and STAC (location shown in c)). Note that STAC is a pseudo-site name assigned to stacked time series of TRPD and BN05 (See text and Figure S6 for details). Black dots at the bottom panel indicate magnitude of detected seismicity. Notable large earthquakes are marked with stars, epicenters of which are shown in c). b) Same as a) but with data between 30 days before and after the mainshock. A moving median with a window length of 24 hours is shown in blue for each site. c) Site location (red inverted triangles) and epicenters (stars with corresponding colors with a) and b)). The same figure is shown in Figure S9 for north displacement.

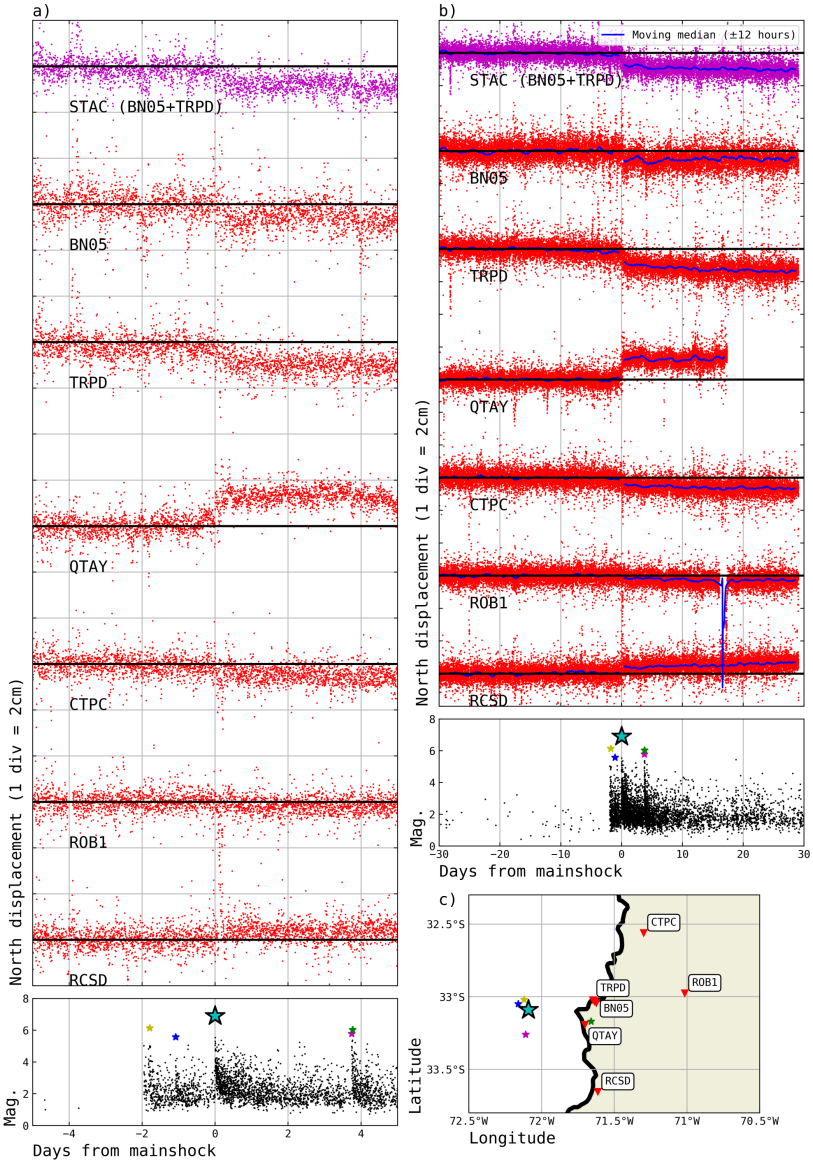

Figure S7. Same as Figure S6 but for north displacements.

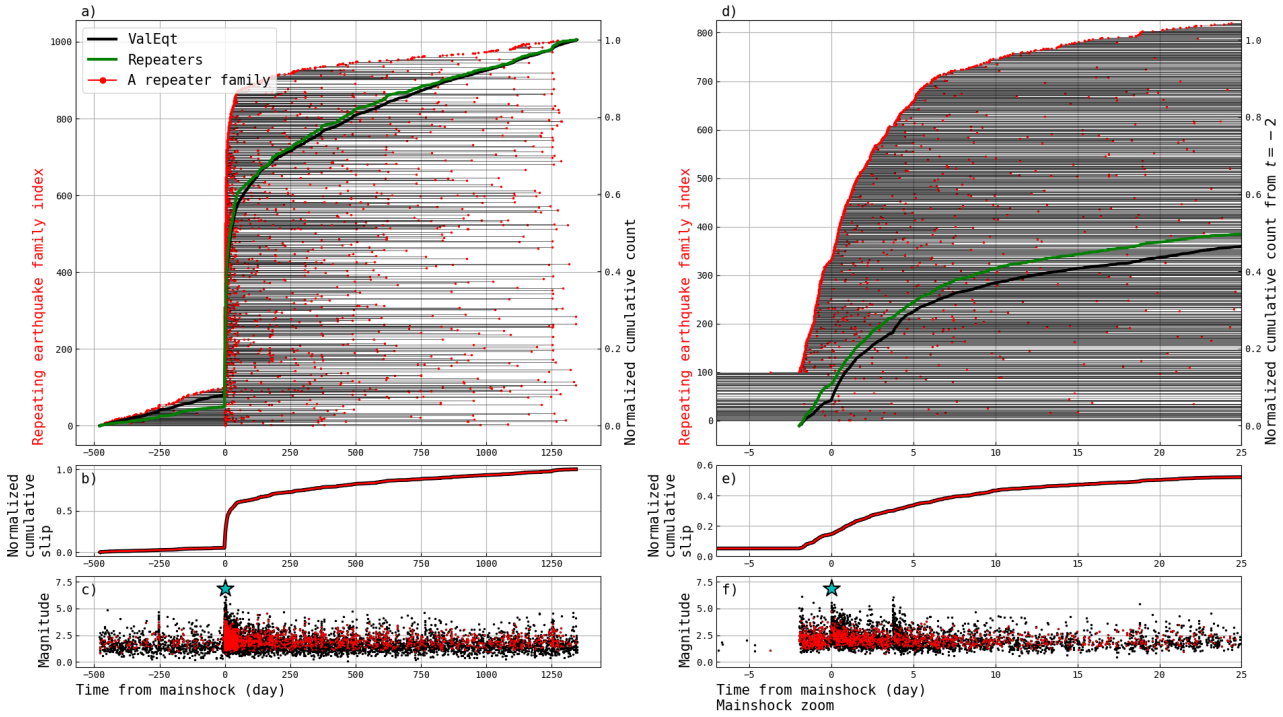

Figure S8. (a) Families of repeating earthquake detected in the ValEqt catalog but using a cross-correlation window centered only on the P phase. A horizontal black line represent one family by connecting the repeating earthquake (red dots). The green and black curves is the normalized cumulative number of repeaters and ValEqt earthquakes respectively. (b) Normalized cumulative slip estimated from repeating earthquakes. (c) Times and magnitudes of ValEqt earthquakes (black dot) and repeating earthquakes (red dot). The blue star indicate the mainshock. (d, e and f) Same as (a, b and c) but zoomed in the vicinity of the mainshock time. Note that the normalized cumulative count of repeaters and ValEqt earthquake start at t=-2 days in (d).

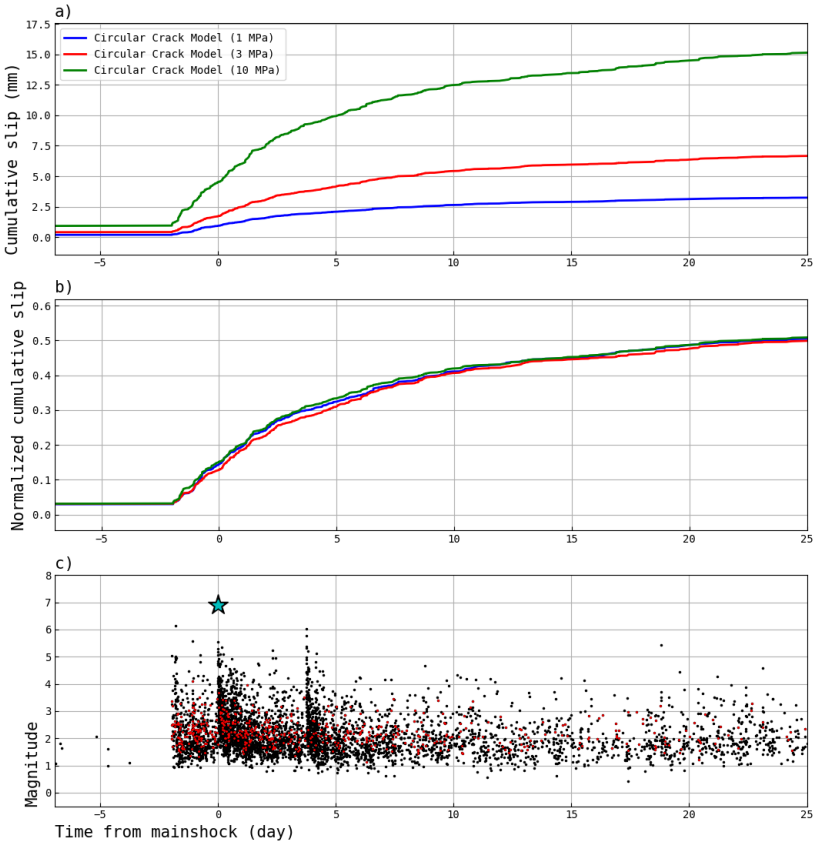

Figure S9. Aseismic slip estimate from repeating earthquakes as function of Stress Drop (Circular Crack model). (a) Absolute slip estimate. (b) Normalized slip estimate. (c) Times and magnitudes of ValEqt earthquakes (black dot) and repeating earthquakes (red dot). The blue star indicate the mainshock.